

000 EGOMEM: LIFELONG MEMORY AGENT FOR FULL- 001 DUPLEX OMNIMODAL MODELS 002

003 **Anonymous authors**
004

005 Paper under double-blind review
006

007 ABSTRACT 008

009 We introduce EgoMem, the first lifelong memory agent tailored for full-duplex
010 models that process real-time omnimodal streams. EgoMem enables real-time
011 models to recognize different users from raw audiovisual streams, to provide person-
012 alized response, and to maintain long-term knowledge of users' facts, preferences,
013 and social relationships extracted from audiovisual history. EgoMem operates with
014 three asynchronous processes: (i) a *retrieval* process that dynamically identifies
015 user via face and voice, and gathers relevant context from a long-term memory; (ii)
016 an *omnimodal dialog* process that generates personalized audio responses based
017 on the retrieved context; and (iii) a *memory management* process that automatically
018 detects dialog boundaries from omnimodal streams, and extracts necessary
019 information to update the long-term memory. Unlike existing memory agents for
020 LLMs, EgoMem relies entirely on raw audiovisual streams, making it especially
021 suitable for lifelong, real-time, and embodied scenarios. Experimental results
022 demonstrate that EgoMem's retrieval and memory management modules achieve
023 over 95% accuracy on the test set. When integrated with a fine-tuned RoboEgo
024 omnimodal chatbot, the system achieves fact-consistency scores above 87% in
025 real-time personalized dialogs, establishing a strong baseline for future research.
026

027 1 INTRODUCTION 028

029 A wide range of AI applications involve lifelong omnimodal streams. A notable example is a robot
030 deployed in homes and public spaces (AgiBot-World-Contributors et al., 2025; Bu et al., 2025). In
031 similar scenarios, the models are required not only to follow instructions swiftly, but also to recognize
032 users, remember their histories, understand social relationships, and deliver personalized services.
033 Technically, the crucial capabilities to meet these requirements include *omnimodality*, *real-time*
034 *responsiveness*, and *humanoid cognition* (Wang & Sun, 2025). For *real-time responsiveness*, there
035 have been solutions to achieve full duplexity, either based on time-division multiplexing (Wang et al.,
036 2024; Zhang et al., 2024b), or on native duplex (Défossez et al., 2024; Yao et al., 2025a) schemes. Yet,
037 *humanoid cognition* remains an underexplored capability for current omnimodal, full-duplex systems.
038 In this work, we study the lifelong memory capability as a critical step towards *humanoid cognition*,
039 since memory is the foundation of both human and advanced artificial intelligence (Jimenez Gutierrez
040 et al., 2024). We focus on real-time personalized dialog as a major task to validate the effectiveness
041 of lifelong memory in omnimodal scenarios.
042

043 We showcase the role of lifelong memory in personalized omnimodal dialogs as follows. (1) When a
044 user Emily shows up, a polling process detects the user identity as Emily directly from the audiovisual
045 stream (e.g., camera and microphone inputs); (2) The profile of Emily is encoded and put into the
046 dialog context of an omnimodal chatbot; (3) When Emily asks "does any of my colleagues love tennis?",
047 a query regarding the relation "colleague" and keyword "tennis" is generated by the chatbot, activating
048 a textual retrieval to the knowledge base containing Emily's social relation graph, which returns a
049 dialog record of "John, colleague, 2024-05-13, user discussed a tennis game he played 2 days ago". This
050 record is further encoded as dialog context; (4) The chatbot answers "Yes, Emily, your colleague John
051 loves tennis" based on the available context; (5) The system extracts user facts: "Emily shows interest in
052 tennis", and dialog record "2024-05-14, user asked if any of her colleagues loves tennis.", from the raw
053 audiovisual stream of the recent dialog, and updates Emily's profile memory with these contents for
future use; (6) When Emily shows up on another day, the model is able to greet with: "Hi Emily, did you
talk to John about tennis?".

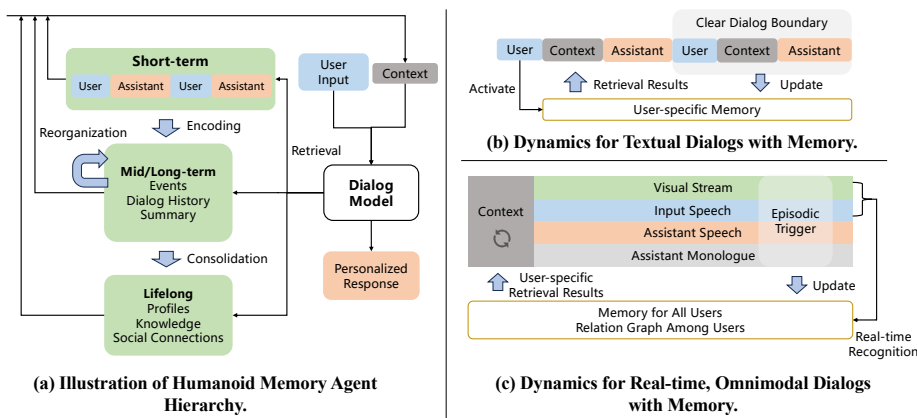


Figure 1: Textual memory agents vs. full-duplex omnimodal memory (ours).

In literature, two primary approaches have been explored to equip textual large language models (LLMs) with long-term memory: extended context windows (Su et al., 2021; Wu et al., 2024) and memory agents (Zhong et al., 2024; Chhikara et al., 2025; Xu et al., 2025b; Kang et al., 2025). However, neither method transfers well to *lifelong omnimodal* scenarios. On one hand, extended context windows can retain long sequences encoding full omnimodal information (He et al., 2024). Yet, in lifelong settings, the length of audiovisual streams grows without bound, making even million-token contexts insufficient (Men et al., 2024). On the other hand, memory agent methods (Figure 1 (a)) are well-suited for lifelong operation (Lee et al., 2024; Wang & Chen, 2025; Li et al., 2025b), but typically rely on several strong assumptions: user identities are explicitly known, dialog sessions have clear boundaries, and all inputs are textual (Figure 1 (b)). Unfortunately, these assumptions do not hold in full-duplex omnimodal applications (Défossez et al., 2024; Zhang et al., 2024a; Lin et al., 2025), in which the user identities are implicitly encoded in audiovisual streams, and there is no well-defined boundaries for dialog turns or user sessions (Figure 1 (c)). Furthermore, existing memory agents generally overlook the multiuser social relation graph (Au et al., 2025), which is an important element for humanoid cognition in lifelong scenarios.

To address these issues, we propose EgoMem, the first lifelong memory system tailored for omnimodal scenarios and designed to facilitate full-duplex personalized dialog. EgoMem operates through three asynchronous processes. First, a **Retrieval Process** is responsible for real-time polling recognition of users, implemented with an audiovisual retrieval mechanism. It also contains a content-driven text retrieval module to gather related textual documents. This process facilitates efficient integration of both user-specific and RAG-style (Gao et al., 2023) information into the dialog flow. Second, an **Omnimodal Dialog Process** uses a fine-tuned dialog model to deliver full-duplex, personalized responses in real time, grounded in the retrieved context. Third, a **Memory Management Process** handles dialog boundary detection, information extraction, and memory updating, based on real-time raw audiovisual streams. This process ensures up-to-date memory over time.

We integrate EgoMem memory system to RoboEgo (Yao et al., 2025b), a *native* full-duplex model that is best aligned with our target scenarios. We fine-tune RoboEgo under our EgoMem framework to deliver real-time, lifelong, and personalized responses to arbitrary user. We conduct automated evaluations across the audio, textual, and visual retrieval modules, the memory management module, and the system’s personalization abilities, considering either single-user profile (Level-1) and multi-user social graph (Level-2) as reference contexts. Evaluation results show that these modules exhibit high accuracy and robustness, and that the incorporation of EgoMem enhances personalization without compromising RoboEgo’s original dialog capabilities.

Our contributions are as follows: (1) *framework*: we propose EgoMem, a lifelong memory agent for full-duplex, omnimodal interaction, which to the best of our knowledge is the first of its kind; (2) *implementation*: we provide a concrete implementation of EgoMem based on the RoboEgo backbone, including detailed module designs, data construction pipelines, and training configurations; (3) *evaluation*: we demonstrate that EgoMem achieves robust performance on personalization tasks in lifelong omnimodal scenarios, establishing a solid baseline for future research.

108

2 PRELIMINARIES

109

2.1 FULL-DUPLEX OMNIMODAL MODELS

110 Full-duplex omnimodal models are able to process real-time audiovisual inputs and demonstrate
 111 capabilities to listen and speak simultaneously. In each time step t , a full-duplex omnimodal model
 112 F takes as input a listening audio a_t , video frames v_t , and optionally a textual input l_t . It generates a
 113 slice of spoken audio response r_t :

$$114 \quad r_t = F_\theta(a_t, v_t, l_t). \quad (1)$$

115 We adopt RoboEgo (Yao et al., 2025b) as our primary dialog model, as it supports a *native* full-duplex
 116 scheme at least for audio. The *native* scheme features lower response latency and better scalability
 117 (Défossez et al., 2024; Lin et al., 2025; Yao et al., 2025a), compared to time-division multiplexing
 118 (TDM) schemes. Also, in general instruction-following tasks, RoboEgo’s response quality and user
 119 experiences are comparable to state-of-the-art systems such as Qwen-2.5-Omni (Xu et al., 2025a).

120 In RoboEgo, both the listening and speaking stream are processed with a frame rate of 12.5 fps, each
 121 frame corresponding to one autoregressive forward step t . In each step, 17 tokens are merged into one
 122 embedding: the listening and speaking audio frame are both encoded by 8 tokens, and the text channel
 123 contributes 1 token. Please refer to Appendix A for more details on the model’s structure and stream
 124 organization. Note that EgoMem’s framework and methodology can be applied to other full-duplex
 125 omnimodal models F or to different organizations of a_t , v_t , and l_t beyond our implementation.

126

2.2 MEMORY AGENT PARADIGM

127 EgoMem is designed to facilitate full-duplex, personalized chat for lifelong-deployed omnimodal
 128 models. As a first step, we focus on the case where there is only one active speaker at a time, leaving
 129 the more complex cocktail party problem (Haykin & Chen, 2005) for future work. In this setting,
 130 in each time step t , the main dialog model F takes two additional inputs: the user profile p_t , and
 131 reference information c_t :

$$132 \quad r_t = F_\theta(a_t, v_t, l_t, p_t, c_t). \quad (2)$$

133 Here, p_t and c_t are encoded in the text channel, commonly referred to as the *context* or *short-term*
 134 *memory* in current literature, delivered to F as part of its KV-cache (Vaswani et al., 2017; Dao, 2023).

135 EgoMem manages a textual memory M with three core functions: *retrieval*, *writing*, and *updating*.

136 *Retrieval*. The retrieval function provides p_t and c_t to the dialog model by searching related information
 137 in M based on current dialog content:

$$138 \quad p_t, c_t = \text{EgoMem.retr}(a_t, v_t, M). \quad (3)$$

139 In traditional textual memory agents (Gao et al., 2023), p_t is naively accessible from user accounts,
 140 while the retrieval process for c_t is always activated after the user’s textual input. In lifelong
 141 omnimodal scenarios, however, both user identities and dialog boundaries are implicit. The memory
 142 agent should directly detect user identities and session boundaries from raw audiovisual streams.

143 *Writing*. The writing function extracts important events from lifelong multimodal streams and stores
 144 them in the memory unit M :

$$145 \quad \text{Episode} = \text{EgoMem.extract}(a_{0 \sim t}, v_{0 \sim t}, l_{0 \sim t}), \quad (4)$$

$$146 \quad M \leftarrow \text{EgoMem.write}(M, \text{Episode}). \quad (5)$$

147 In EgoMem, memory writing is asynchronous to the main dialog, executed through independent
 148 processes. Unlike traditional memory agents, EgoMem takes as input the raw multimodal stream
 149 fragments in the dialog history (“episodic memory”), and extracts textual descriptions for the events,
 150 user persona, and other useful information.

151 *Updating*. EgoMem periodically performs online or offline memory consolidation: it integrates
 152 existing memory into new, consolidated representations, and solves potential conflicts:

$$153 \quad M \leftarrow \text{EgoMem.update}(M). \quad (6)$$

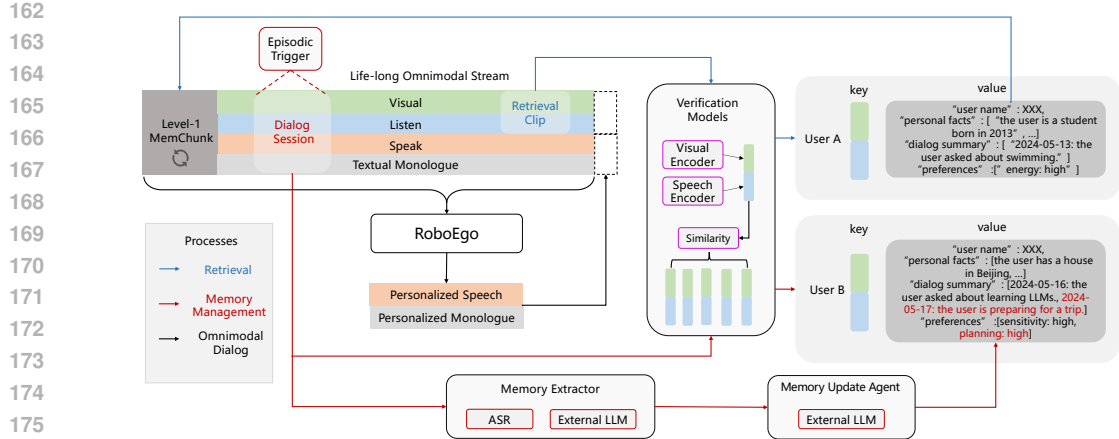


Figure 2: System illustration for EgoMem Level-1 (Profile-only).

3 EGO MEM

The design of EgoMem can be divided to two levels: Level-1 EgoMem facilitates profile-based personalization; and Level-2 EgoMem supports additional references such as users’ social networks. Compared to Level-1, Level-2 is particularly suited for application scenarios where users are more interconnected, such as home robots. We introduce the implementation of each level based on our dialog flow outlined in Section 2.1.

3.1 LEVEL-1 EGO MEM: PROFILE-ONLY

In Level-1, M contains only the profile information for each of its recognized users. Formally, it sets $c_t = \text{None}$ in equations 2 and 3. The profile of each user in a key-value pair: the *key* contains one visual embedding v_f^u for face verification and one audio embedding v_s^u for speaker verification; the *value* is a dictionary storing the users’ name, personal facts, summary of previous dialogs, and preferences. The operation flow of Level-1 EgoMem is illustrated in Figure 2. It is driven by the three component processes running asynchronously: the *retrieval* process (Section 3.1.1), the *omnimodal dialog* process (Section 3.1.2), and the *memory management* process (Section 3.1.3).

3.1.1 RETRIEVAL

To identify the current user, a retrieval process runs in a lifelong “polling” manner with fixed intervals of 2 seconds. This is a critical design enabling the dialog model to *actively start* talking to the user (e.g., “Greetings John!”). In every 2 seconds, EgoMem processes a chunk of audio and visual signals with length τ , and extracts query vectors:

$$v_f^q = \text{visual_encoder}(v_{(t-\tau):t}), \quad (7)$$

$$v_s^q = \text{speech_encoder}(a_{(t-\tau):t}). \quad (8)$$

v_f^q and v_s^q are used for face and speaker verification with each *user*’s key (v_f^u and v_s^u), respectively. If a valid user is found, its profile is tokenized with a textual tokenizer and pushed to the textual channel of a special *Level-1 MemChunk* field in the main dialog’s token stream (Figure 2, top left). This special chunk occupies a maximum length of 512 time steps, with its 16 audio tokens always filled with `<empty>`. It is attended by every forward pass of the RoboEgo model. Note that *Level-1 MemChunk* is managed exclusively by the retrieval process: its textual content is refreshed only when the current recognized user differs from the previous one. Every time *Level-1 MemChunk* is refreshed, EgoMem triggers one additional forward pass for RoboEgo that updates the KV cache for the entire dialog history. This operation introduces ignorable overhead in inference.

Face Verification. We leverage an open-sourced pipeline from DeepFace (Serengil & Ozpinar, 2024) to extract faces from video frames. Specifically, we use Retinaface (Deng et al., 2020) as

216 a face detection backend, and Facenet512 (Schroff et al., 2015) as the visual encoder, resulting in
 217 512-dimensional face features. The retrieval quits if no face is detected; otherwise, we first find the
 218 closest existing user u with the minimal cosine distance $d = 1 - \text{cosine_similarity}(v_f^q, v_f^u)$ to the
 219 query vector v_f^q , and then verify with a pre-tuned threshold $\delta = 0.3$:
 220

$$\text{current user} = \begin{cases} u, & \text{if } d < \delta, \\ \text{new user}, & \text{else.} \end{cases} \quad (9)$$

224 **Speaker Verification.** We leverage a wavelm_large (Chen et al., 2022) model fine-tuned specifically
 225 for speaker verification (Anastassiou et al., 2024) as our speech feature extractor, producing 256-
 226 dimensional v_s^q and v_s^u vectors. We combine cosine similarity with adaptive s-norm (Karam et al.,
 227 2011; Cumani et al., 2011) for best performance and robustness (Section 5.1).
 228

229 3.1.2 OMNIMODAL DIALOG

231 This is the main process running the RoboEgo chat service. *Level-1 MemChunk* is attended by
 232 RoboEgo in each step. If no user profile is returned by the retrieval process, *Level-1 MemChunk*'s text
 233 channel is filled with $\langle\text{pad}\rangle$ tokens. We fine-tune RoboEgo with the corresponding streaming data
 234 format (Section 4) to generate personalized spoken responses based on the user's profile information.
 235

236 3.1.3 MEMORY MANAGEMENT

237 The *memory management* process instantiates EgoMem's extract, write, and update functions (eq. 4 - 6).
 238 With a fixed time interval, it conducts content extraction on the 17-way audio-language token stream
 239 from the main dialog process. For a 8192-step stream chunk (~ 11 minutes) in history, each time step
 240 is labeled by a sequence tagging model (namely **Episodic Trigger**) to mark the boundaries of dialog
 241 sessions for each user. Next, an external LLM, serving as **Memory Extractor**, is prompted to extract
 242 events, user facts, and user preferences from the fragmented streams of each session. Afterwards, the
 243 memory management process calls the retrieval functions to identify the user of this session. If a
 244 *new* user is found, EgoMem creates a new memory item in M , stores the face/speech embedding as
 245 keys, and initializes the user's profile with the extracted contents. Otherwise, the user identity and the
 246 extracted memory contents are provided to a **Memory Update Agent**, which is an external LLM
 247 prompted to figure out potential conflicts and update the user's profile in M .
 248

249 **Episodic Trigger.** The episodic trigger is used to find the boundaries of dialog sessions in which the
 250 user's identity is consistent. It not only detects the start and end of dialog sessions, but also splits the
 251 sessions from different users. Specifically, the episodic trigger predicts tags for each time step in the
 252 audio stream (the aligned listen and speak audio tokens):
 253

$$\text{Tag}_{0 \sim t} = \text{episodic_trigger}(a_{0 \sim t}, r_{0 \sim t}). \quad (10)$$

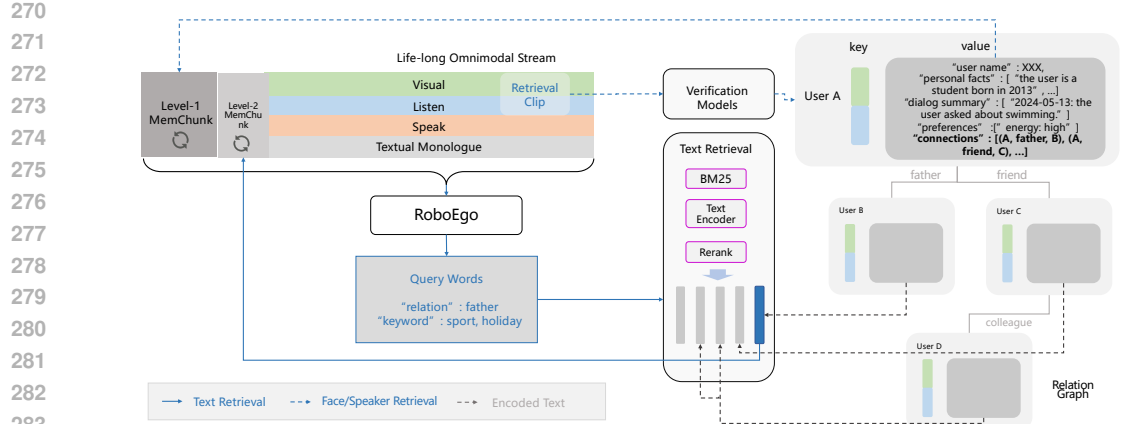
254 Specifically, the episodic trigger assigns a label to each time step with the following paradigm: {0:
 255 *no dialog*; 1: *start of a new user's dialog session*; 2: *in-session step*; 3: *end of current user's session*}.
 256 The detailed model structure is explained in Appendix B.1.
 257

258 The **Memory Extractor** and **Memory Update Agent** are also detailed in Appendix B.1.
 259

260 3.2 LEVEL-2 EGOMEM: CONTENT-DRIVEN

261 In Level-2 EgoMem, M maintains not only the user profiles, but also the social relation graph among
 262 them. For each user, we add a field containing a list of triplets representing the graph edges from the
 263 current user to others. Optionally, any other useful information can be added to M for a similar RAG
 264 processes. Formally, Level-2 EgoMem provides both p_t and c_t in equations 2 and 3. While p_t comes
 265 from a *polling* user recognition, c_t comes from the the primary model (RoboEgo)'s *active* retrieval
 266 to M . We exemplify Level-2 EgoMem in Figure 3, showing its major differences to Level-1. We
 267 specify the comparison to Level-1 for each of the core processes (Section 3.1.1 - 3.1.3) as follows:
 268

269 **Level-2 Retrieval.** As shown in Figure 3, the *Level-1 MemChunk* maintains its function in the
 270 Level-2 system; it is driven by the external polling retrieval process. An *Level-2 MemChunk* with



270
271
272
273
274
275
276
277
278
279
280
281
282
283
284
285 **Figure 3: System illustration for EgoMem Level-2 (Content-driven).** We focus on showing the
286 differences in retrieval process and hide the details for other processes like memory management.
287

288 a maximum length of 256 is added to the reserved field in the stream; unlike *Level-1 MemChunk*,
289 *Level-2 MemChunk* is driven by active textual queries from the RoboEgo dialog model. For example,
290 in a dialog session between user A and RoboEgo, *Level-1 MemChunk* is kept the same (user A’s
291 profile). In contrast, after each user instruction, RoboEgo can activate an independent **Textual**
292 **Retrieval** process to memory M . A textual query is generated by RoboEgo on its monologue channel
293 based on the current dialog. The retrieval result is tokenized and cached in *Level-2 MemChunk*. The
294 implementation of this **Textual Retrieval** sub-module is provided in Appendix B.2.

295 **Level-2 Omnimodal Dialog.** In Level-2, the primary dialog model is allowed to actively generate
296 textual queries in arbitrary time. Specifically, we fine-tune RoboEgo to generate two groups of query
297 words formatted as $<\text{retr}>:\text{n}<\text{group1}>\text{n}<\text{group2}><\text{answer}>$, with group1 being the “relation query” and
298 group2 being the “keyword query”. Each group is a sequence of query words separated by comma.
299 When the final $<\text{answer}>$ token is generated, EgoMem activates a textual retrieval process to update
300 the *Level-2 MemChunk*. The training process is introduced in Section 4.

301 **Level-2 Memory Management.** The only differences to Level-1 include the **Memory Extractor** is
302 prompted to also extract new *relation* facts from the raw dialog contents (e.g., User A says he is the
303 boyfriend of User B now), and the **Memory Update Agent** is prompted to link the user to existing
304 users accordingly, updating the edges of the social graph.

306 4 TRAINING APPROACH

309 We fine-tune RoboEgo to generate personalized response with Level-1/2 EgoMem. We also train the
310 Episodic Trigger to label the dialog boundary for memory extraction. Interestingly, the data collection
311 for these three tasks can be unified by different *supervision masks* on the same token stream.

313 4.1 DATA COLLECTION

315 **Audio Dialogs.** We collect textual transcripts simulating the lifelong personalized scenarios utilizing
316 both Level-1 and Level-2 EgoMem. We synthesize user profiles and social graphs, collect open-
317 sourced dialog datasets, and generate ground-truth personalized answers using large (visual-)language
318 models. The textual transcripts are converted to audiovisual dialogs using text-to-speech (TTS)
319 models, followed by audio augmentation to improve robustness. Details are provided in Appendix C.

321 **Token Stream Organization.** Multiple dialog sessions from different users are tokenized and
322 concatenated, forming *token streams*. With a probability of 0.3, a later user instruction *interrupts*
323 an ongoing model response, simulating the most widely-considered full-duplex scenario. The
concatenated waveform are tokenized with a Mimi tokenizer (Défossez et al., 2024), formatted

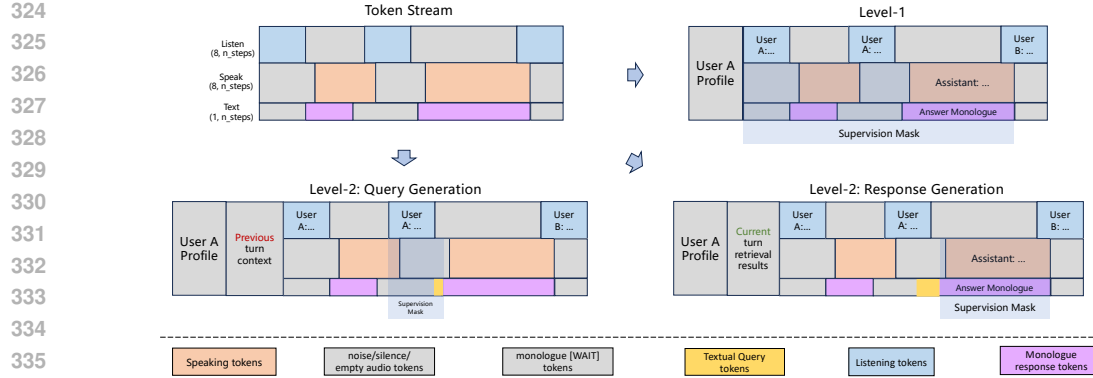


Figure 4: Token stream structure and supervision mask for EgoMem training data.

as described in Appendix A, and truncated to a maximum length of 8192 steps. For the textual monologue channel, we record the actual start point of each audio response, and position the textual response tokens to start 2 steps earlier. We follow the *natural* monologue strategy (Yao et al., 2025a) instead of applying word-level alignment between text and audio (Défossez et al., 2024). For each training sample with 8192 steps, positions 0-511 are reserved for the *Level-1 MemChunk*, and positions 512-768 for the *Level-2 MemChunk*, with dialogs beginning after these reserved slots. Figure 4 (top left) illustrates our token stream organization.

4.2 TRAINING WITH SUPERVISION MASKS

We apply three different kinds of *supervision masks* on the token streams introduced above, supporting the following three tasks:

For *Level-1 EgoMem*, for each of the N multi-turn dialogs in a token stream, we position the corresponding user's profile in *Level-1 MemChunk*, and set the supervision mask to 1 for the textual and speak tokens only in the time span of the corresponding dialog, and 0 for other time steps, producing N distinct training samples in total (Figure 4, top right).

For *Level-2 EgoMem*, more fine-grained supervision mask is applied to each turn $t_i, i \in [0, T_j]$ for each dialog $d_j, j \in [0, N]$ in a token stream. Specifically, for query word generation, we maintain the content of *Level-1 MemChunk* and *Level-2 MemChunk* for the previous turn, position the ground-truth query words right before the textual response for current turn, and set supervision mask to 1 from the audio start point of the current turn until the end of query words span (Figure 4, bottom left). For personalized response generation, we conduct textual retrieval with the ground-truth query words, gather the supporting fact from the connected users in the relation graph, and fill them into the *Level-2 MemChunk*. *Level-1 MemChunk* is filled with current user profile. With these contexts, we supervise on the textual and speaking tokens from the end of query words to the audio end point of dialog, including the full response utterance (Figure 4, bottom right). To summarize, for each turn, the query words and personalized response are supervised separately with different contexts, yielding $2 * \sum_{i=0}^N T_j$ distinct training samples from each token stream.

For *Episodic Trigger*, we leverage a full supervision mask. Each time step in the token stream is labeled following the paradigm in Section 3.1.3.

The training configurations for the above three tasks are introduced in Appendix D.

5 EXPERIMENTS

We focus on the following three research questions: (1) Do our retrieval sub-modules correctly identify users and recall the relevant contents? (2) Does the episodic trigger detect the correct boundaries of multimodal dialogs? (3) Does the fine-tuned RoboEgo model effectively leverage the Level-1 and Level-2 EgoMem to deliver lifelong personalized responses? We answer these questions with quantitative results on dedicated benchmarks. As the first work in lifelong memory agents for

378 **Table 1:** Face verification, speaker recognition, and text retrieval results for EgoMem sub-modules.
379

380 381 382 383 384 385 386 387 388 389 390 391 392 393 394 395 396 397 398 399 400 401 402 403 404 405 406 407 408 409 410 411 412 413 414 415 416 417 418 419 420 421 422 423 424 425 426 427 428 429 430 431	380 381 382 383 384 385 386 387 388 389 390 391 392 393 394 395 396 397 398 399 400 401 402 403 404 405 406 407 408 409 410 411 412 413 414 415 416 417 418 419 420 421 422 423 424 425 426 427 428 429 430 431	Face Verification	Speaker Recognition			Text Retrieval
		Metrics	Accuracy	pass@1 w/o s-norm	pass@1 w/ s-norm	EER
Results	0.984	0.958	0.965	0.00892	0.960	
Elapsed time (s)	0.2		0.1		0.1	

full-duplex omnimodal systems, we will also release part of our test set for personalized omnimodal dialog generation to benefit future research.

5.1 RETRIEVAL EVALUATION

We present the benchmark and settings to evaluate the retrieval capabilities for EgoMem. The retrieval results are summarized in Table 1.

Face Verification. We benchmark the face retrieval module on the Labeled Faces in the Wild (LFW, (Huang et al., 2008)) dataset, achieving an accuracy of 98.4%, which is consistent with public results¹. As the open-sourced solution demonstrates satisfying face verification performance and robustness to variations in pose and angle, we directly integrate it in our system without additional fine-tuning. The face retrieval module processes one query within 0.2 seconds with a single Nvidia H100 GPU.

Speaker Verification. We construct our evaluation benchmark from the public VoxCeleb (Nagrani et al., 2017) speaker verification dataset. To enable adaptive s-norm (Karam et al., 2011; Cumani et al., 2011) which is widely agreed to benefit the task, we leverage SeedTTS-eval (Anastassiou et al., 2024) as the source of imposter cohorts, using 1,000 Chinese speech embeddings as the candidate cohort set for the queries, and 2,000 embeddings for the keys. We set up a cohort number of 200 (i.e., for both the queries and the keys, the 200 closest utterances in the candidate cohorts are used to compute the mean and variance statistics for adaptive s-norm).

To assess the impact of adaptive s-norm, we first synthesize a retrieval task with 1,000 query utterances and 120 key utterances from different speakers in VoxCeleb, and compare the pass@1 with or without adaptive s-norm. We observe a moderate improvement from 95.8% to 96.5% with adaptive s-norm, confirming its benefit for retrieval stability.

Next, we sample a more challenging speaker verification test set from VoxCeleb with a highly imbalanced ratio of positive (same-speaker) to negative (different-speaker) pairs of 1:119, yielding 5,000 samples in total. Our speaker verification module achieves an Equal Error Rate (EER) of 0.89% on this benchmark with a decision threshold of 4.63. For deployment, we adjust the threshold to 6 based on human case studies to balance precision and recall. The whole speaker verification system takes less than 0.1 seconds for a retrieval run with more than 1,000 candidate entries.

Text Retrieval. In Level-2 EgoMem, text retrieval is used to gather relevant information w.r.t the relation and keyword queries. We therefore focus on the pass@5 metric, as it measures the ability of the system to return all relevant facts within a textual window shorter than 256 tokens (the size of the *Level-2 MemChunk*). We construct a benchmark of 200 queries sampled from our personalized dialog transcripts, with a candidate entry pool of 500 (relation, personal fact) texts. Using the straightforward retrieval strategy described in Appendix B.2, the system achieves a pass@5 score of 96%. The full system latency is controlled to be under 0.1s with a single Nvidia H100 GPU.

5.2 EPISODIC TRIGGER EVALUATION

We hold out a test set from the collected token streams (Section 4.1) for episodic trigger evaluation, containing 1,000 samples. We use two types of metrics: (1) *Jaccard score* measuring the overlap of dialog session spans; (2) *span_match@N* which measures precision, recall, and F1 scores for detected dialog boundaries, allowing a tolerance of $\pm N$ steps from the ground truth.

¹<https://github.com/serengil/deepface/tree/master/benchmarks>

432
433
434
435
436
437
438
439
440
441
442
443
444
445
446
447
448
449
450
451
452
453
454
455
456
457
458
459
460
461
462
463
464
465
466
467
468
469
470
471
472
473
474
475
476
477
478
479
480
481
482
483
484
485**Table 2:** Episodic trigger evaluation results.

Metrics	Jaccard	P/R/F1@0	P/R/F1@5	P/R/F1@10	Elapsed time (s)
Clean	0.992	0.857/0.857/0.857	0.986/0.986/0.986	0.986/0.986/0.986	
Noised	0.989	0.790/0.788/0.789	0.983/0.981/0.982	0.984/0.982/0.983	0.08

Table 3: Personalized dialog evaluation results.

Models	Level-1			Level-2		
	Fact Score	Answer Quality	Throughput (fps)	Fact Score	Answer Quality	Throughput (fps)
Clean	0.959	9.170	21.73	0.895	8.970	20.56
Noised	0.931	9.020		0.876	8.820	

The results are presented in Table 2. At $N = 5$, our episodic trigger achieves an F1 score of more than 0.98 under both clean and noised environments, indicating robust “Valid Audio Detection” (VAD) and user session splitting capabilities within a deviation of less than ($5/12.5 = 0.4$) seconds. Notably, noisy environments can significantly affect the prediction of more fine-grained boundaries (i.e., less than 0.2s), as we observe a large gap on $span_match@0$. This is intuitive since it takes time to figure out whether a voice indicates the start of a new user’s session or just another period of noise. The episodic trigger takes 0.08 seconds to annotate a 10-minute chunk with 8192 time steps.

5.3 PERSONALIZED DIALOG EVALUATION

We hold out a test set from the masked token streams (Section 4.1) to assess the quality of personalized responses produced by RoboEgo, integrated with Level-1 and Level-2 EgoMem. For each dialog turn, we provide an evaluator model with the following inputs: the user instruction (textual transcript), the ground-truth textual response, the contents of the *MemChunks*, and the textual monologue response generated by RoboEgo. The evaluator is implemented with the DeepSeek-V3 API, prompted to return two scores: (1) *Fact Score*: A binary 0/1 metric for each turn indicating whether the model’s response is personalized to the user and consistent with the user profile, without factual errors. (2) *Answer Quality*: A score from 0 to 10 for each turn measuring the general helpfulness and quality of the response with respect to the user instruction, regardless of personalization.

We present the results in Table 3. We observe that for both Level-1 and Level-2 EgoMem, the models successfully achieve the expected RAG capability based on the retrieval results present in *MemChunks*. RoboEgo achieves lower *Fact Score* in the Level-2 task, largely due to more frequent *MemChunk* updates and error cascading from the textual retrieval module. For the *Answer Quality* scores which are independent of the retrieval results, the gap becomes smaller, indicating that neither Level-1 nor Level-2 EgoMem significantly degrades the base instruct-following capability of RoboEgo.

We observe a slight drop in throughput with Level-2 memory as it introduces a longer *MemChunk*. Yet, this latency is negligible in the user experiences of full-duplex real-time chatting, as the model generates audio frames in more than 20 fps, significantly exceeding the minimum requirement for real-time audio decoder (12.5 fps).

6 CONCLUSION AND FUTURE CHALLENGES

In this work, we explored lifelong memory for full-duplex omnimodal models. We first defined the task and outlined the core functions, and then introduced our proposed memory system, EgoMem: Level-1 (profile-based) and Level-2 (content-driven). We integrated EgoMem to the omnimodal dialog model, RoboEgo, as an implementation example. Experimental results demonstrate that, for the first time, an omnimodal dialog agent can be equipped with robust lifelong personalization capabilities, establishing a strong baseline to support future research. Due to computational constraints, we did not explore larger model sizes or more advanced functionalities, such as complex tool use. Future directions include extending the profile/graph memory to encompass procedural memory and multimodal contents, as well as investigating whether trainable parameters can replace some of the complex agent modules and memory units.

486
487
ETHICS STATEMENT488
489
490
491
492
The data used to train the three tasks supporting our EgoMem agent is derived from synthetic
transcripts generated by publicly accessible large language models. No real-world users are involved
in this process, and no privacy is compromised during data collection. EgoMem is a plug-in
methodology that can be applied to a wide range of models. The content generated by the dialog
models does not reflect the views or opinions of the authors or affiliated institutions.493
494
REPRODUCIBILITY STATEMENT
495496
497
498
499
500
We provide comprehensive details of the system paradigm, implementation, and training config-
urations in Sections 2, 3, 4, as well as in the Appendix. We will release a portion of our test set
along with the associated code for stream organization, inference, and evaluation. The functions and
signals used in Level-1 and Level-2 EgoMem are clearly defined, which we believe will support the
community in reproducing our agent system and developing future variants.501
502
REFERENCES
503504
505
506
507
508
509
510
511
512
513
AgiBot-World-Contributors, Qingwen Bu, Jisong Cai, Li Chen, Xiuqi Cui, Yan Ding, Siyuan Feng,
Shenyuan Gao, Xindong He, Xu Huang, Shu Jiang, Yuxin Jiang, Cheng Jing, Hongyang Li, Jialu
Li, Chiming Liu, Yi Liu, Yuxiang Lu, Jianlan Luo, Ping Luo, Yao Mu, Yuehan Niu, Yixuan Pan,
Jiangmiao Pang, Yu Qiao, Guanghui Ren, Cheng Ruan, Jiaqi Shan, Yongjian Shen, Chengshi
Shi, Mingkang Shi, Modi Shi, Chonghao Sima, Jianheng Song, Huijie Wang, Wenhao Wang,
Dafeng Wei, Chengen Xie, Guo Xu, Junchi Yan, Cunbiao Yang, Lei Yang, Shukai Yang, Maoqing
Yao, Jia Zeng, Chi Zhang, Qinglin Zhang, Bin Zhao, Chengyue Zhao, Jiaqi Zhao, and Jianchao
Zhu. Agibot world colosseo: A large-scale manipulation platform for scalable and intelligent
embodied systems. *CoRR*, abs/2503.06669, 2025. doi: 10.48550/ARXIV.2503.06669. URL
<https://doi.org/10.48550/arXiv.2503.06669>.514
515
516
517
518
519
520
521
522
Philip Anastassiou, Jiawei Chen, Jitong Chen, Yuanzhe Chen, Zhuo Chen, Ziyi Chen, Jian Cong,
Lelai Deng, Chuang Ding, Lu Gao, Mingqing Gong, Peisong Huang, Qingqing Huang, Zhiying
Huang, Yuanyuan Huo, Dongya Jia, Chumin Li, Feiya Li, Hui Li, Jiaxin Li, Xiaoyang Li, Xingxing
Li, Lin Liu, Shouda Liu, Sichao Liu, Xudong Liu, Yuchen Liu, Zhengxi Liu, Lu Lu, Junjie Pan,
Xin Wang, Yuping Wang, Yuxuan Wang, Zhen Wei, Jian Wu, Chao Yao, Yifeng Yang, Yuanhao
Yi, Junteng Zhang, Qidi Zhang, Shuo Zhang, Wenjie Zhang, Yang Zhang, Zilin Zhao, Dejian
Zhong, and Xiaobin Zhuang. Seed-tts: A family of high-quality versatile speech generation
models. *CoRR*, abs/2406.02430, 2024. doi: 10.48550/ARXIV.2406.02430. URL <https://doi.org/10.48550/arXiv.2406.02430>.523
524
525
526
Steven Au, Cameron J Dimacali, Ojasmitra Pedirappagari, Namyong Park, Franck Dernoncourt,
Yu Wang, Nikos Kanakaris, Hanieh Deilamsalehy, Ryan A Rossi, and Nesreen K Ahmed. Per-
sonalized graph-based retrieval for large language models. *arXiv preprint arXiv:2501.02157*,
2025.527
528
529
530
Tom Brown, Benjamin Mann, Nick Ryder, Melanie Subbiah, Jared D Kaplan, Prafulla Dhariwal,
Arvind Neelakantan, Pranav Shyam, Girish Sastry, Amanda Askell, et al. Language models are
few-shot learners. *Advances in neural information processing systems*, 33:1877–1901, 2020.531
532
533
Qingwen Bu, Jisong Cai, Li Chen, Xiuqi Cui, Yan Ding, Siyuan Feng, Shenyuan Gao, Xindong
He, Xuan Hu, Xu Huang, et al. Agibot world colosseo: A large-scale manipulation platform for
scalable and intelligent embodied systems. *arXiv preprint arXiv:2503.06669*, 2025.534
535
536
537
Jianlv Chen, Shitao Xiao, Peitian Zhang, Kun Luo, Defu Lian, and Zheng Liu. Bge m3-embedding:
Multi-lingual, multi-functionality, multi-granularity text embeddings through self-knowledge
distillation. *arXiv preprint arXiv:2402.03216*, 2024a.538
539
Lin Chen, Jinsong Li, Xiaoyi Dong, Pan Zhang, Yuhang Zang, Zehui Chen, Haodong Duan, Jiaqi
Wang, Yu Qiao, Dahua Lin, et al. Are we on the right way for evaluating large vision-language
models? *arXiv preprint arXiv:2403.20330*, 2024b.

540 Sanyuan Chen, Chengyi Wang, Zhengyang Chen, Yu Wu, Shujie Liu, Zhuo Chen, Jinyu Li, Naoyuki
 541 Kanda, Takuya Yoshioka, Xiong Xiao, et al. Wavlm: Large-scale self-supervised pre-training
 542 for full stack speech processing. *IEEE Journal of Selected Topics in Signal Processing*, 16(6):
 543 1505–1518, 2022.

544 Prateek Chhikara, Dev Khant, Saket Aryan, Taranjeet Singh, and Deshraj Yadav. Mem0: Building
 545 production-ready ai agents with scalable long-term memory. *arXiv preprint arXiv:2504.19413*,
 546 2025.

547 Sandro Cumani, Pier Domenico Batzu, Daniele Colibro, Claudio Vair, Pietro Lafase, Vasileios
 548 Vasilakakis, et al. Comparison of speaker recognition approaches for real applications. In
 549 *Interspeech*, pp. 2365–2368, 2011.

550 Tri Dao. Flashattention-2: Faster attention with better parallelism and work partitioning. *arXiv*
 551 *preprint arXiv:2307.08691*, 2023.

552 Alexandre Défossez, Laurent Mazaré, Manu Orsini, Amélie Royer, Patrick Pérez, Hervé Jégou,
 553 Edouard Grave, and Neil Zeghidour. Moshi: a speech-text foundation model for real-time dialogue.
 554 *CoRR*, abs/2410.00037, 2024. doi: 10.48550/ARXIV.2410.00037. URL <https://doi.org/10.48550/arXiv.2410.00037>.

555 Jiankang Deng, Jia Guo, Evangelos Ververas, Irene Kotsia, and Stefanos Zafeiriou. Retinaface:
 556 Single-shot multi-level face localisation in the wild. In *Proceedings of the IEEE/CVF conference*
 557 *on computer vision and pattern recognition*, pp. 5203–5212, 2020.

558 Jacob Devlin, Ming-Wei Chang, Kenton Lee, and Kristina Toutanova. BERT: pre-training of
 559 deep bidirectional transformers for language understanding. In Jill Burstein, Christy Doran, and
 560 Thamar Solorio (eds.), *Proceedings of the 2019 Conference of the North American Chapter of*
 561 *the Association for Computational Linguistics: Human Language Technologies, NAACL-HLT*
 562 *2019, Minneapolis, MN, USA, June 2–7, 2019, Volume 1 (Long and Short Papers)*, pp. 4171–
 563 4186. Association for Computational Linguistics, 2019. doi: 10.18653/v1/n19-1423. URL
 564 <https://doi.org/10.18653/v1/n19-1423>.

565 Alexey Dosovitskiy, Lucas Beyer, Alexander Kolesnikov, Dirk Weissenborn, Xiaohua Zhai, Thomas
 566 Unterthiner, Mostafa Dehghani, Matthias Minderer, Georg Heigold, Sylvain Gelly, et al. An
 567 image is worth 16x16 words: Transformers for image recognition at scale. *arXiv preprint*
 568 *arXiv:2010.11929*, 2020.

569 Harishchandra Dubey, Ashkan Aazami, Vishak Gopal, Babak Naderi, Sebastian Braun, Ross Cutler,
 570 Hannes Gamper, Mehrsa Golestaneh, and Robert Aichner. Icassp 2023 deep noise suppression
 571 challenge. In *ICASSP*, 2023.

572 Yunfan Gao, Yun Xiong, Xinyu Gao, Kangxiang Jia, Jinliu Pan, Yuxi Bi, Yixin Dai, Jiawei Sun,
 573 Haofen Wang, and Haofen Wang. Retrieval-augmented generation for large language models: A
 574 survey. *arXiv preprint arXiv:2312.10997*, 2(1), 2023.

575 Gemini. Gemini 1.5: Unlocking multimodal understanding across millions of tokens of context.
 576 *arXiv preprint arXiv:2403.05530*, 2024.

577 Simon Haykin and Zhe Chen. The cocktail party problem. *Neural computation*, 17(9):1875–1902,
 578 2005.

579 Bo He, Hengduo Li, Young Kyun Jang, Menglin Jia, Xuefei Cao, Ashish Shah, Abhinav Shrivastava,
 580 and Ser-Nam Lim. Ma-lmm: Memory-augmented large multimodal model for long-term video
 581 understanding. In *Proceedings of the IEEE/CVF Conference on Computer Vision and Pattern*
 582 *Recognition*, pp. 13504–13514, 2024.

583 Gary B Huang, Marwan Mattar, Tamara Berg, and Eric Learned-Miller. Labeled faces in the wild:
 584 A database for studying face recognition in unconstrained environments. In *Workshop on faces*
 585 *in 'Real-Life' Images: detection, alignment, and recognition*, 2008.

586 Bernal Jimenez Gutierrez, Yiheng Shu, Yu Gu, Michihiro Yasunaga, and Yu Su. Hipporag: Neurobio-
 587 logically inspired long-term memory for large language models. *Advances in Neural Information*
 588 *Processing Systems*, 37:59532–59569, 2024.

594 Jiazheng Kang, Mingming Ji, Zhe Zhao, and Ting Bai. Memory os of ai agent. [arXiv preprint](https://arxiv.org/abs/2506.06326)
 595 [arXiv:2506.06326](https://arxiv.org/abs/2506.06326), 2025.

596

597 Zahi N Karam, William M Campbell, and Najim Dehak. Towards reduced false-alarms using cohorts.
 598 In [2011 IEEE international conference on acoustics, speech and signal processing \(ICASSP\)](#), pp.
 599 4512–4515. IEEE, 2011.

600

601 Kuang-Huei Lee, Xinyun Chen, Hiroki Furuta, John Canny, and Ian Fischer. A human-inspired
 602 reading agent with gist memory of very long contexts. [arXiv preprint arXiv:2402.09727](https://arxiv.org/abs/2402.09727), 2024.

602

603 Jia-Nan Li, Jian Guan, Songhao Wu, Wei Wu, and Rui Yan. From 1,000,000 users to every user:
 604 Scaling up personalized preference for user-level alignment. [arXiv preprint arXiv:2503.15463](https://arxiv.org/abs/2503.15463),
 605 2025a.

606

607 Zhiyu Li, Shichao Song, Hanyu Wang, Simin Niu, Ding Chen, Jiawei Yang, Chenyang Xi, Huayi
 608 Lai, Jihao Zhao, Yezhaohui Wang, et al. Memos: An operating system for memory-augmented
 609 generation (mag) in large language models. [arXiv preprint arXiv:2505.22101](https://arxiv.org/abs/2505.22101), 2025b.

610

611 Shijia Liao, Yuxuan Wang, Tianyu Li, Yifan Cheng, Ruoyi Zhang, Rongzhi Zhou, and Yijin Xing.
 612 Fish-speech: Leveraging large language models for advanced multilingual text-to-speech synthesis,
 613 2024. URL <https://arxiv.org/abs/2411.01156>.

613

614 Guan-Ting Lin, Jiachen Lian, Tingle Li, Qirui Wang, Gopala Anumanchipalli, Alexander H. Liu, and
 615 Hung yi Lee. Full-duplex-bench: A benchmark to evaluate full-duplex spoken dialogue models on
 616 turn-taking capabilities, 2025. URL <https://arxiv.org/abs/2503.04721>.

617

618 Aixin Liu, Bei Feng, Bing Xue, Bingxuan Wang, Bochao Wu, Chengda Lu, Chenggang Zhao,
 619 Chengqi Deng, Chenyu Zhang, Chong Ruan, et al. Deepseek-v3 technical report. [arXiv preprint](https://arxiv.org/abs/2412.19437)
 619 [arXiv:2412.19437](https://arxiv.org/abs/2412.19437), 2024.

620

621 Mary L McHugh. Interrater reliability: the kappa statistic. [Biochemia medica](#), 22(3):276–282, 2012.

622

623 Xin Men, Mingyu Xu, Bingning Wang, Qingyu Zhang, Hongyu Lin, Xianpei Han, and Weipeng
 624 Chen. Base of rope bounds context length. [arXiv preprint arXiv:2405.14591](https://arxiv.org/abs/2405.14591), 2024.

624

625 Leann Myers and Maria J Sirois. Spearman correlation coefficients, differences between.
 626 [Encyclopedia of statistical sciences](#), 12, 2004.

627

628 Arsha Nagrani, Joon Son Chung, and Andrew Zisserman. Voxceleb: a large-scale speaker identifica-
 629 tion dataset. [arXiv preprint arXiv:1706.08612](https://arxiv.org/abs/1706.08612), 2017.

630

631 Stephen Robertson, Hugo Zaragoza, et al. The probabilistic relevance framework: Bm25 and beyond.
 632 [Foundations and Trends® in Information Retrieval](#), 3(4):333–389, 2009.

632

633 Florian Schroff, Dmitry Kalenichenko, and James Philbin. Facenet: A unified embedding for face
 634 recognition and clustering. In [Proceedings of the IEEE conference on computer vision and pattern](#)
 635 [recognition](#), pp. 815–823, 2015.

636

637 Philip Sedgwick. Pearson’s correlation coefficient. [Bmj](#), 345, 2012.

638

639 Sefik Serengil and Alper Ozpinar. A benchmark of facial recognition pipelines and co-usability
 640 performances of modules. [Journal of Information Technologies](#), 17(2):95–107, 2024. doi:
 641 10.17671/gazibtd.1399077. URL [https://dergipark.org.tr/en/pub/gazibtd/](https://dergipark.org.tr/en/pub/gazibtd/issue/84331/1399077)
 641 issue/84331/1399077.

642

643 Jianlin Su, Yu Lu, Shengfeng Pan, Bo Wen, and Yunfeng Liu. Roformer: Enhanced transformer with
 644 rotary position embedding. [CoRR](#), abs/2104.09864, 2021. URL <https://arxiv.org/abs/2104.09864>.

645

646 Ashish Vaswani, Noam Shazeer, Niki Parmar, Jakob Uszkoreit, Llion Jones, Aidan N Gomez, Łukasz
 647 Kaiser, and Illia Polosukhin. Attention is all you need. [Advances in neural information processing](#)
 647 [systems](#), 30, 2017.

648 Peng Wang, Songshuo Lu, Yaohua Tang, Sijie Yan, Yuanjun Xiong, and Wei Xia. A full-duplex
 649 speech dialogue scheme based on large language models. *CoRR*, abs/2405.19487, 2024. doi: 10.
 650 48550/ARXIV.2405.19487. URL <https://doi.org/10.48550/arXiv.2405.19487>.
 651

652 Yequan Wang and Aixin Sun. Toward embodied agi: A review of embodied ai and the road ahead.
 653 [arXiv preprint arXiv:2505.14235](https://arxiv.org/abs/2505.14235), 2025. URL <https://arxiv.org/abs/2505.14235>.
 654

655 Yu Wang and Xi Chen. Mirix: Multi-agent memory system for llm-based agents. [arXiv preprint
 656 arXiv:2507.07957](https://arxiv.org/abs/2507.07957), 2025.
 657

658 Bingyang Wu, Shengyu Liu, Yinmin Zhong, Peng Sun, Xuanzhe Liu, and Xin Jin. Loongserve:
 659 Efficiently serving long-context large language models with elastic sequence parallelism. In
 660 *Proceedings of the ACM SIGOPS 30th Symposium on Operating Systems Principles*, pp. 640–
 661 654, 2024.
 662 X.AI. Realworldqa, 2024. URL <https://x.ai/blog/grok-1.5v>.
 663

664 Can Xu, Qingfeng Sun, Kai Zheng, Xiubo Geng, Pu Zhao, Jiazhan Feng, Chongyang Tao, and
 665 Daxin Jiang. Wizardlm: Empowering large language models to follow complex instructions.
 666 *CoRR*, abs/2304.12244, 2023. doi: 10.48550/arXiv.2304.12244. URL <https://doi.org/10.48550/arXiv.2304.12244>.
 667

668 Jin Xu, Zhifang Guo, Jinzheng He, Hangrui Hu, Ting He, Shuai Bai, Keqin Chen, Jialin Wang, Yang
 669 Fan, Kai Dang, et al. Qwen2. 5-omni technical report. [arXiv preprint arXiv:2503.20215](https://arxiv.org/abs/2503.20215), 2025a.
 670

671 Wujiang Xu, Kai Mei, Hang Gao, Juntao Tan, Zujie Liang, and Yongfeng Zhang. A-mem: Agentic
 672 memory for llm agents. [arXiv preprint arXiv:2502.12110](https://arxiv.org/abs/2502.12110), 2025b.
 673

674 Dongchao Yang, Jinchuan Tian, Xu Tan, Rongjie Huang, Songxiang Liu, Xuankai Chang, Jiatong
 675 Shi, Sheng Zhao, Jiang Bian, Xixin Wu, et al. Uniaudio: An audio foundation model toward
 676 universal audio generation. [arXiv preprint arXiv:2310.00704](https://arxiv.org/abs/2310.00704), 2023.
 677

678 Yiqun Yao, Xiang Li, Xin Jiang, Xuezhi Fang, Naitong Yu, Wenjia Ma, Aixin Sun, and Yequan Wang.
 679 Flm-audio: Natural monologues improves native full-duplex chatbots via dual training. [arXiv
 680 preprint arXiv:2509.02521](https://arxiv.org/abs/2509.02521), 2025a.
 681

682 Yiqun Yao, Xiang Li, Xin Jiang, Xuezhi Fang, Naitong Yu, Aixin Sun, and Yequan Wang. Roboego
 683 system card: An omni-modal model with native full duplexity. [arXiv preprint arXiv:2506.01934](https://arxiv.org/abs/2506.01934),
 684 2025b.
 685

686 Qinglin Zhang, Luyao Cheng, Chong Deng, Qian Chen, Wen Wang, Siqi Zheng, Jiaqing Liu, Hai
 687 Yu, Chaohong Tan, Zhihao Du, et al. Omnidflatten: An end-to-end gpt model for seamless voice
 688 conversation. [arXiv preprint arXiv:2410.17799](https://arxiv.org/abs/2410.17799), 2024a.
 689

690 Xinrong Zhang, Yingfa Chen, Shengding Hu, Xu Han, Zihang Xu, Yuanwei Xu, Weilin Zhao,
 691 Maosong Sun, and Zhiyuan Liu. Beyond the turn-based game: Enabling real-time conversations
 692 with duplex models. [arXiv preprint arXiv:2406.15718](https://arxiv.org/abs/2406.15718), 2024b.
 693

694 Hanyu Zhao, Li Du, Yiming Ju, Chengwei Wu, and Tengfei Pan. Beyond iid: Optimizing instruction
 695 learning from the perspective of instruction interaction and dependency. 2024. URL <https://arxiv.org/abs/2409.07045>.
 696

697 Wanjun Zhong, Lianghong Guo, Qiqi Gao, He Ye, and Yanlin Wang. Memorybank: Enhancing large
 698 language models with long-term memory. In *Proceedings of the AAAI Conference on Artificial
 699 Intelligence*, volume 38, pp. 19724–19731, 2024.
 700

701 Yongxin Zhu, Dan Su, Liqiang He, Linli Xu, and Dong Yu. Generative pre-trained speech language
 702 model with efficient hierarchical transformer. In *Proceedings of the 62nd Annual Meeting of the
 703 Association for Computational Linguistics (Volume 1: Long Papers)*, pp. 1764–1775, 2024.
 704

702 A INTRODUCTION TO THE ROBOEGO MODEL

704 For audio signals a_t , we use the Mimi tokenizer² to extract features at 12.5 frames per second. Each
 705 audio frame is represented by one semantic token and seven acoustic tokens. The audio input and
 706 output are divided into two channels, *listening* and *speaking*, while textual monologue tokens are
 707 placed in an additional textual channel. Thus, . They are additively merged into the input embedding.
 708 The model then processes all the historical input embeddings with a 7B LLM backbone to generate
 709 the hidden state for the current time step. Following the RQ-Transformer architecture (Yang et al.,
 710 2023; Zhu et al., 2024), a lightweight *depth* Transformer (with 100M parameters) first generates a
 711 textual monologue token based on the current hidden state on the top layer, and then generates eight
 712 speaking tokens autoregressively. In lifelong deployment scenarios, this process runs continuously
 713 in real time, forming the main dialog stream, while visual signals v_t are encoded through a Visual
 714 Transformer (Dosovitskiy et al., 2020) and added into the context in a time-division multiplex (TDM)
 715 manner, at fixed intervals of 2–4 seconds. We refer the readers to the related work (Yao et al., 2025b;
 716 Défossé et al., 2024; Yao et al., 2025a) for detailed structural configurations.

717 B EXTRA DETAILS FOR EGOMEM SUB-MODULES

718 B.1 LEVEL-1 SUB-MODULES

722 **Episodic Trigger.** The episodic trigger is an RQ-Transformer-based (Défossé et al., 2024) model
 723 which shares the input stream organization and model structure topology with RoboEgo (Section
 724 2.1), despite being much smaller with 100M parameters. It consumes the 17 audio-text channels
 725 with a maximum time step of 8192 as input. Instead of generating dialog responses, it assigns a
 726 label to each time step with the following paradigm: {0: *no dialog*; 1: *start of a new user’s dialog*
 727 *session*; 2: *in-session step*; 3: *end of current user’s session*}. We modify the attention mask from
 728 a GPT-like (Brown et al., 2020) causal mask to a Bert-like (Devlin et al., 2019) full mask, as the
 729 sequence labeling process is offline and chunk-wise. The training configurations of episodic trigger
 730 is detailed in Section 4. The evaluation results are presented in Section 5.2.

731 **Memory Extractor.** The memory extractor is implemented as the following pipeline:

- 732 • The episodic trigger labels each time step. According to the labels, audio chunks starting
 733 with label “1”, ending with label “3”, and correctly filled with “2” are considered as the
 734 audio source for one user’s dialog session. The corresponding audio waveforms are clipped.
- 735 • The clipped waveform in the listening channel goes through automatic speech recognition
 736 (ASR). Raw ASR results are fed into the memory extractor. The response texts from the
 737 monologue text channel of the dialog model are also provided as reference.
- 738 • We leverage a DeepSeek-V3 (Liu et al., 2024) API to extract meaningful contents to store
 739 in the memory. Specifically, we prompt the model to summarize the dialog content with
 740 short, precise sentences, generate sentences describing the facts about the user, and figure
 741 out a 90-dimensional personal trail (Li et al., 2025a; Kang et al., 2025) for the user. The
 742 user name (or “unknown_user”) is stored in a separate field.

744 **Memory Update Agent.** This is a DeepSeek-V3 API prompted to solve profile conflicts and
 745 formalize the extracted contents from the memory extractor, making sure that they are suitable for
 746 updating the structured memory storage.

748 B.2 LEVEL-2 SUBMODULES

750 **Textual Retrieval.** The textual retrieval system gathers the top-K relevant textual information
 751 according to the query words generated by RoboEgo, and updates the content of *Level-2 MemChunk*.
 752 Specifically, for each user U connected to current user A in the social graph, U ’s name and relation
 753 with A are concatenated with each of U ’s memory items (facts, dialog history, etc.) to form one
 754 candidate document for retrieval. If the “relation query” group is not empty, we first match all relevant

755 ²<https://huggingface.co/kyutai/mimi>

756 users’ documents via the BM25 (Robertson et al., 2009) algorithm using only the relation queries;
 757 next, if the “keyword query” group is not empty, we concatenate all the keyword into one string, and
 758 re-rank the retrieved documents based on their vector distances to this keyword string. We leverage
 759 the BGE-small (Chen et al., 2024a) model as the textual encoder. The top-K results are returned to
 760 the textual channel of *Level-2 MemChunk*.

762 C DATA COLLECTION DETAILS

764 **Textual Transcripts** For *Level-1 EgoMem*, we first use DeepSeek-V3 (Liu et al., 2024) to synthesize
 765 500 user profiles including name, dialog history, and a 90-dimensional persona. Next, we synthesize
 766 10k dialogs between user and AI assistant based on open-source instruct-following datasets (e.g.,
 767 Infinity-Instruct (Zhao et al., 2024), WizardLM (Xu et al., 2023), and multimodal question answering
 768 datasets involving visual inputs (Chen et al., 2024b; X.AI, 2024)): the user instructions are retained,
 769 while responses are refined by DeepSeek-V3 (or Gemini-2.5-Pro (Gemini, 2024) for VQA) to be
 770 more helpful and personalized. Finally, we prompt DeepSeek-V3 to include more question styles
 771 in which users ask questions regarding their own dialog history and profiles. Each dialog typically
 772 contains 3–5 turns.

773 **For Level-2 EgoMem**, we first synthesize 500 possible relations (e.g., “father”, “colleague”), construct
 774 relation graphs linking one main user with 3–5 socially connected users. We prompt DeepSeek-V3 to
 775 generate questions requiring relation-graph reasoning (e.g., “Does my mother like physical exercise?”)
 776 and mix these questions with general instructions, producing 5k dialogs. For each question, the model
 777 annotates the effective query words (including both relation query and keywords query, both can be
 778 empty) sufficient to retrieve supporting facts from the profiles of connected users. After generating
 779 the query words, the model should also provide the ground-truth personalized response for training.

780 **TTS and Augmentation.** Audio dialogs are synthesized from the collected transcripts. Each user
 781 utterance is assigned a random human voice, and converted into speech with Fishaudio TTS (Liao
 782 et al., 2024), while model responses are consistently generated with a single fixed voice. For the
 783 listening channel, we add diverse noise from sources like DNS Challenge (Dubey et al., 2023) and
 784 RNNNoise³, as well as random speech clips. Following Moshi (Défossez et al., 2024), we also simulate
 785 microphone echo by mixing the speaking channel into the listening channel with probability 0.3,
 786 applying random gain (0–0.2x) and delay (0.1–0.5s).

788 D TRAINING DETAILS

790 **For Level-1 EgoMem**, we fine-tune RoboEgo with a dataset containing 158K samples with different
 791 (*Level-1 MemChunk*, token stream context, supervision mask) combinations. We duplicate the
 792 dataset by using both the original and noise-augmented listening channel. Training starts from one
 793 of RoboEgo’s SFT checkpoints, running for 5 epochs with batch size 64 and a cosine learning rate
 794 decay from 1e-5 to 1.5e-6.

795 **For Level-2 EgoMem**, RoboEgo is fine-tuned on 54K samples with valid *Level-2 MemChunk* and the
 796 corresponding query words, combined with 50% of the Level-1 training dataset reformatted with
 797 empty *Level-2 MemChunk* and query words. As with Level-1, the dataset is duplicated with clean
 798 and noisy listening channels. Training resumes from the same RoboEgo checkpoint as in Level-1,
 799 running for 1 epoch with batch size 64 and a cosine learning rate decay from 1e-5 to 1.5e-6.

800 **For Episodic Trigger**, the sequence tagging model is initialized randomly. We train the model with
 801 100K clean samples and 100K noised samples. The number of epoch is set to 45. We use a batch size
 802 of 64 and the learning rate decays from 1e-4 to 1e-6 following a cosine schedule.

803
 804
 805
 806
 807
 808
 809
³<https://github.com/xiph/rnnoise>

810 E REBUTTAL REVISION
811812 This section addresses common concerns raised during the review process.
813814 E.1 REAL-WORLD DEMO CASE
815816 We provide a 2-minute anonymous video (link: <https://figshare.com/s/ebd3210db6b0a47149b7>) demonstrating the performance of a deployed version of EgoMem
817 in real-world multimodal chatting, which showcases the generalization capabilities from synthetic
818 training to real-world application.
819820 E.2 JUSTIFICATION OF LLM EVALUATION
821822 **Correlation with Human Scores.** To assess the alignment between our LLM-based scoring and
823 human judgment, we recruited graduate students specializing in AI to annotate model responses
824 on a 50-turn subset of our test set. Evaluators were provided only with the initial prompts used for
825 the model API and were instructed to assign Level-2 fact/quality scores based on the established
826 guidelines. We computed Cohen’s Kappa (McHugh, 2012) coefficient for the Fact Score as it is cate-
827 gorical, and the Pearson (Sedgwick, 2012) and Spearman (Myers & Sirois, 2004) coefficients for the
828 Answer Quality scores. These metrics are standard metrics for validating evaluation methodologies.
829 We averaged the coefficients across different annotators. The results are presented in Table 4. We
830 observe all coefficients exceed 0.6, indicating a strong positive correlation between LLM and human
831 evaluations.
832833 **Table 4:** Alignment analysis between LLM and human scores.
834

Fact Score		Answer Quality	
Kappa	Pearson	Spearman	
0.683	0.621	0.624	

835 E.3 ROBUSTNESS IN REAL-WORLD ENVIRONMENTS
836837 **Human Evaluation with Real-world Audiovisual Dialogs (no-memory).** While there is substantial
838 agreement between LLM and human evaluations regarding Fact Score and Answer Quality, we
839 acknowledge concerns regarding the robustness and user experience of a model trained on synthetic
840 data. To address this, we conducted a comparative analysis with Qwen-2.5-omni in real-world audio
841 dialogs, employing the same human evaluation metrics used in the backbone model (Yao et al.,
842 2025b). We observe that EgoMem maintains a competitive advantage in key metrics related to the
843 audio chatting experience, including Naturalness, Responsiveness, and Robustness. Notably: (i) as
844 Qwen-2.5-omni lacks memory capabilities, we evaluated using random daily queries rather than
845 memory-dependent ones; and (ii) the helpfulness score is significantly higher than that reported by
846 RoboEgo, which is attributed to the differing difficulty distributions of the instructions. These results,
847 combined with our demo video, demonstrate that training on synthesized data yields robust dialog
848 experiences.
849850 **Table 5:** Comparison to Qwen-2.5-omni on multimodal dialogs in real-world environments.
851

Model	Helpfulness	Naturalness	Responsiveness	Robustness
Qwen-2.5-omni	8.2	8.0	8.2	7.7
RoboEgo+memory	8.1	8.1	8.7	8.2

852 E.4 ABLATION/CLARIFICATION ON THE SUB-MODULES’ ROLES
853854 We clarify the role of different sub-modules with ablation studies when necessary.
855856 **Episodic Trigger vs. Rule-based Session Splitting.** We further clarify the contributions of specific
857 sub-modules through ablation studies.
858

864 **Episodic Trigger vs. Rule-based Session Splitting.** Given the novelty of the Episodic Trigger in our
 865 architecture, we provide additional results to justify its necessity. We selected 30 recorded streams,
 866 each containing multiple dialogs with distinct user voices. We established a baseline session-splitting
 867 solution that relies primarily on the face/voice retrieval system to identify speaker changes and mark
 868 dialog boundaries, subsequently applying overlapping rules to align ASR timestamps with these
 869 boundaries.

870 We compared this baseline against our proposed memory extraction pipeline utilizing the Episodic
 871 Trigger. The extracted memory from each stream was subjected to a blind win-tie-lose human
 872 annotation. The results are summarized in Table 6.

873 **Table 6:** Ablation analysis: Episodic Trigger vs. Rule-based.

Episodic Trigger Wins	Tie	Rule-based Wins
14	10	6

874 **Impact of ASR and External LLM in Memory Extractor.** We evaluate the impact of the ASR
 875 module and the External LLM within the memory extractor using 30 Level-1 stream cases, comparing
 876 the human-annotated Fact Score on immediate factual questions about the extracted content. We test
 877 two ASR systems with different word error rates (WER), each under two conditions: (i) storing raw
 878 ASR transcripts as memory and (ii) using an External LLM to summarize and refine the content.
 879 Results are shown in Table 7.

880 **Table 7:** Ablation analysis: ASR and External LLM.

ASR WER	Fact Score: Raw ASR	Fact Score: EgoMem
5.9	0.73	0.87
3.0	0.87	0.9

881 We observe that when raw ASR transcripts are used directly, the ASR model’s WER significantly
 882 affects the Fact Score, largely due to noisy or missing transcriptions of user instructions. In contrast,
 883 when an External LLM is applied, it jointly analyzes the user’s ASR output and the dialog model’s
 884 monologue—which is typically high-quality once the model correctly interprets the user speech.
 885 Leveraging this dual input, the External LLM effectively repairs imperfect ASR outputs, making the
 886 system more robust to ASR noise and variations across ASR models.

887 **More Clarification on the role of Face/Speaker Verification Modules.** We clarify that the results
 888 presented in Table 3 are based on the test token streams with the ground-truth users, which actually
 889 measures the model’s listening and dialog generation capabilities, as well as the text retrieval quality
 890 for Level-2. If the user identification itself fails, the Fact Score will be zero. Thus, it is reasonable
 891 to directly multiply a 0.96~0.98 scale factor on the Fact Scores to measure the Fact Scores of the
 892 integrated system.

904 E.5 BREAKDOWN ANALYSIS OF BAD CASES

905 We select 50 bad cases in the test corpus of Table 3 and hand-checked the full pipeline for attribution
 906 analysis. As mentioned above, the possible failure modes include incorrect understanding of user
 907 instructs (**Class-1**), failure in recalling relative Level-2 information from textual retrieval (**Class-2**),
 908 and failure in aggregating the MemChunk information into the answer (**Class-3**). The distribution of
 909 the error types are presented in Table 8. The majority of failures comes from the listening and audio
 910 understanding capability, while the memory system itself contributes a smaller portion.

911 **Table 8:** Breakdown analysis of bad cases.

Class-1	Class-2	Class-3
68%	22%	10%